ELECTRODE-LESS PLASMA JET SYNTHESIS OF CORE-SHELL IRON/IRON OXIDE NANOPARTICLES

Jaroslav HNILICA[1], Vít KUDRLE[1], Ondřej JAŠEK[2]

[1] *Masaryk University, Brno, Czech Republic, EU, yaryk@mail.muni.cz*

[2] *CEITEC - Central European Institute of Technology, Masaryk University, Brno, Czech Republic, EU*

Abstract

We report on core-shell iron and iron oxide nanoparticle prepared by plasma synthesis controlled by process gas mixture. The synthesis was carried out using an atmospheric pressure microwave electrodeless plasma jet. We focused on phase composition control and better passivation. We studied the influence of O_2, H_2 and N_2 admixtures to the Ar process gas on the properties of the prepared nanomaterial. Similarly to thermal process, the oxygen admixture preferentially produced Fe_2O_3 nanoparticles whereas hydrogen admixture resulted in particles with higher metallic content. However, in contrast to thermal process, the addition of nitrogen did not produce iron nitride, but iron/iron-oxide core-shell nanoparticles with enhanced chemical stability.

Keywords: core-shell, iron/iron oxide,nanoparticles, electrode-less,

1. INTRODUCTION

In recent years, the interest in iron and iron oxide based nanomaterials (e.g nanoparticles, nanopowders, nanolayers, etc.) is growing due to their Unixe properties. The research and development is truly interdisciplinary: magnetism, catalysis, optics, sorption, biocompatibility, chemical stability, etc. [1, 2, 3].

Nowadays, the iron based nanomaterials are produced commercially using well-established chemical methods, for example co-precipitation, micelles, microemulsion or hydrothermal syntheses. However, these methods often use solvents or surfactants and involve complicated or multistep procedures. As a result, there is a modern trend to replace the wet chemical steps by plasma based technology that could provide an environmentally attractive alternative [4, 5].

A wide range of methods involving plasmas is now available for the preparation of iron-based nanoparticles, e.g. arc discharge, flame synthesis, laser pyrolysis, microwave plasma synthesis and many others. We recently investigated the synthesis of iron oxide nanoparticles in microwave torch discharge [6, 7, 8].

In this paper, we have decided to carry out a similar study using a different, electrodeless design. Moreover, we focused more on influence of working gas composition on the properties of the prepared nanopowders.

2. EXPERIMENTAL

The synthesis of iron based nanoparticles was carried out in atmospheric pressure microwave electrodeless jet – surfatron [9] – from iron pentacarbonyl ($Fe(CO)_5$) mixed with argon. Figure 1 shows the experimental setup. We operated the microwave generator (2.45 GHz) in amplitude modulation mode using a function generator (sinus waveform, 260 Hz frequency) in order to stabilise the plasma discharge. The microwaves were fed to the wave launcher (surfatron) via waveguide, ferrite circulator and coaxial cable. The mean microwave power was maintained at 250 W, whereas the reflecte power was below 10 W. The surfatron device itself (commercial SAIREM Surfatron 80 with integrated matching) exploited a surface wave propagating along plasma boundary to sustain relatively long plasma column. It consisted of coaxial

resonant cavity through which a fused silica discharge tube (80 mm in length, 6 mm and 8 mm inner and outer diameter, respectively) passed.

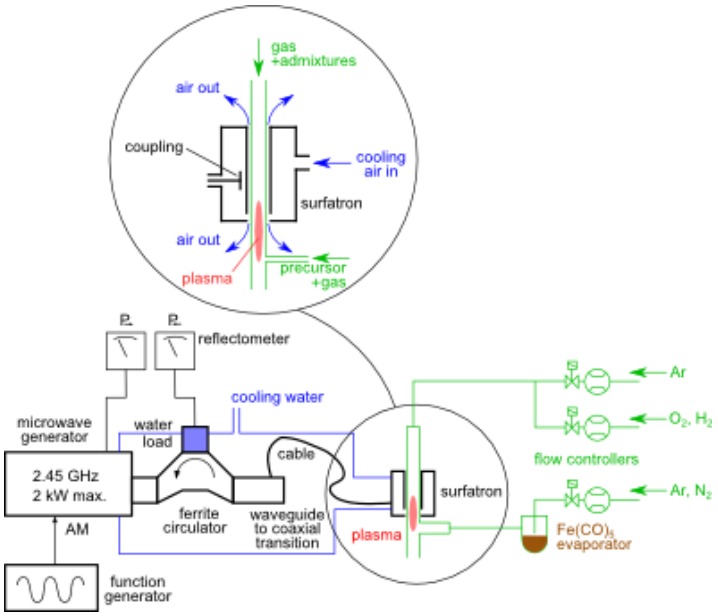

Fig.1 Schematic drawing of the experimental setup

Thermal management was carried out by water cooling of the generator, circulator and surfatron itself. Additionally, the discharge tube was cooled by compressed air.

The flow of working gas, argon, was maintained at 508 sccm by a flow controller. The admixture like O_2 or H_2 (7.3 sccm) could be added into the main inlet upstream from the discharge.

The iron pentacarbonyl $Fe(CO)_5$ liquid precursor (Alfa Aesar, 99.5% purity) was kept in a evaporator and its vapours (0.05 sccm) were transported into the discharge by 100 sccm argon or nitrogen flowing above its surface. The elongated form of a surface wave plasma allowed us to add Fe(CO)5 downstream from the excitation zone, where the active species concentration was still high enough but no conductive deposit was endangering the coupling slit of the surfatron. The nanoparticulate product was collected on the wall of the discharge tube downstream from the mixing tee and on the additional lter. X-ray powder diraction (XRD) was carried out with PANalytical X'Pert Pro MPD device using Co K_α radiation. Raman micro-spectroscopy measurements were performed using Jobin Yvon Labram HR-800 microscope and Renishaw inVia Raman microscope. The spectra were excited with Ar laser (514 nm). The laser power was limited to 1 mW in order to avoid thermally induced phase transformations during the collection of the Raman spectrum. To observe the morphology we used the field emission scanning electron microscope TESCAN Mira 3 in bright field transmitted electron mode.

3. RESULTS AND DISCUSSION

In the following, we discuss the influence of working gas composition on the properties of the prepared nanopowders using three selected experimental conditions. In all cases the main plasma gas was argon at flow-rate 508 sccm and the precursor vapours were introduced at flow rate of 0.05 sccm. Sample S1 was prepared using 7.3 sccm of oxygen admixture to the main gas and 100 sccm of Ar carrying the precursor vapours. Sample S2 was prepared using 7.3 sccm of hydrogen admixture to the main gas and 100 sccm of Ar carrying the precursor vapours. And the sample S3 used 100 sccm of nitrogen to carry the precursor vapours.

Table 1 Composition of the samples as obtained from X-ray diffraction.

Sample	Composition	ICSD No.	d_{XRD} [nm]	wt. [%]
S1	α-Fe_2O_3	82137	59	58
	γ-Fe_2O_3	87119	27	42
S2	α-Fe	53451	39	39
	Fe_3O_4 (+ γ-Fe_2O_3)	75627	18	61
S3	α-Fe	53451	33	74
	Fe_3O_4	75627	13	26

After each synthesis run, the prepared nanopowder was brushed off the discharge tube walls, stored in Eppendorf test tubes and analysed without any further purification or treatment.

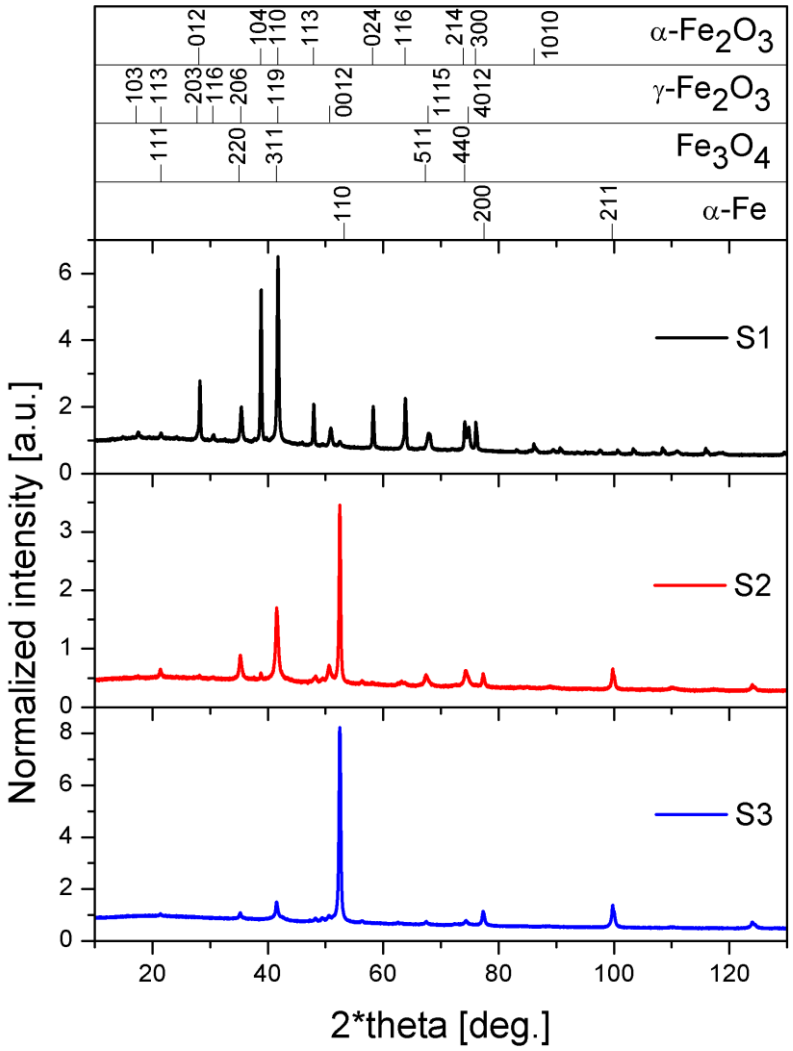

Fig.2 XRD patterns of the synthesised samples for three different gas mixtures. Dominant orientations for relevant iron and iron oxide allomorphs are shown, too

The XRD diffractograms of all three samples are shown in Figure 2. The Rietveld refinement was carried out using software [10] and database [11], giving us the mean coherence length d_{XRD} (crystallite size). The results are summarised in Table 1. The samples consisted of rhombohedral hematite (α-Fe_2O_3), tetragonal maghemite (γ-Fe_2O_3), cubic iron (α-Fe) and cubic magnetite (Fe_3O_4). The mean crystallite size in all samples was in the order of tens of nanometres. It should be noted that XRD of nanopowders has often some

difficulties in distinguishing between magnetite and maghemite. As was suggested in [12], i.e. using the integral (area) of tetragonal maghemite peaks (103), (113), (203), (116) and integral of (111) magnetite peak, we estimate the magnetite to maghemite ratio in sample S2 to be approximately 10:1. In sample S3 no additional maghemite XRD peaks were observed.

The synthesised samples were also analysed by the Raman spectroscopy. Iron oxides, including hematite, maghemite and magnetite, exhibit distinct Raman active phonon modes which can be observed in the measured spectra, see Figure 3.

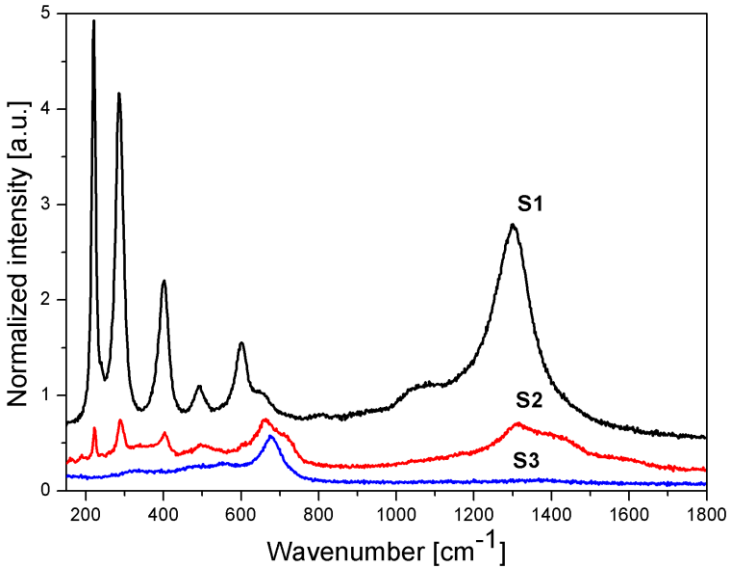

Fig.3 Raman spectra of the synthesised samples for three different gas mixtures

For sample S1 we found strong peaks at 220 and 491 cm^{-1} and lower intensity peaks at 239, 284, 401, 601 and broad peak at 1300 cm^{-1}. These peaks could be attributed to hematite structure, phonon modes 229 (A_{1g}), 249 (E_g), 295 (E_g), 302 (E_g), 414 (E_g), 500 (A_{1g}), 615 (E_g), 660 (longitudinal optical E_u) cm^{-1} [13]. Slight downshift of the mode frequencies could be attributed to influence of the laser power as observed by [14].

Spectra of sample S2 have shown a mixture of hematite, magnetite and maghemite features. Besides the above mentioned strong hematite peaks, we could observe peak at 664 cm^{-1} belonging to magnetite A_{1g} phonon mode and shoulder peak at 713 (A_{1g}) cm^{-1} and above 1400 cm^{-1}, which we assigned to maghemite. The presence of hematite in Raman spectra is in contradiction to XRD analysis and is probably caused by the laser induced change in the sample composition despite a careful procedure and low power setting (1 mW) used in the Raman analysis.

Sample S3 spectra showed intensive peak at 674 cm^{-1} which we assigned to magnetite. Also some broad features in the range of 300 to 600 cm^{-1} could be observed and assigned to magnetite [13]. This result is consistent with our XRD analysis.

The morphology of the synthesized nanopowder was studied using scanning transmission electron microscopy (STEM) mode of scanning electron microscope (SEM). We found roughly spherical nanoparticles of different sizes in the micrograph of the sample S3 (see Figure 4). Both the chains of very small particles (10-15 nm in diameter) and the large particles (more than 20-40 nm in diameter) were found at higher magnifications. Individual α-Fe particles larger than 50 nm as well as the aggregated particles exhibited core-shell morphology. The shell of α-Fe particles is assumed [15] to be formed of Fe_3O_4. The abundance of both materials corresponds to the results from XRD.

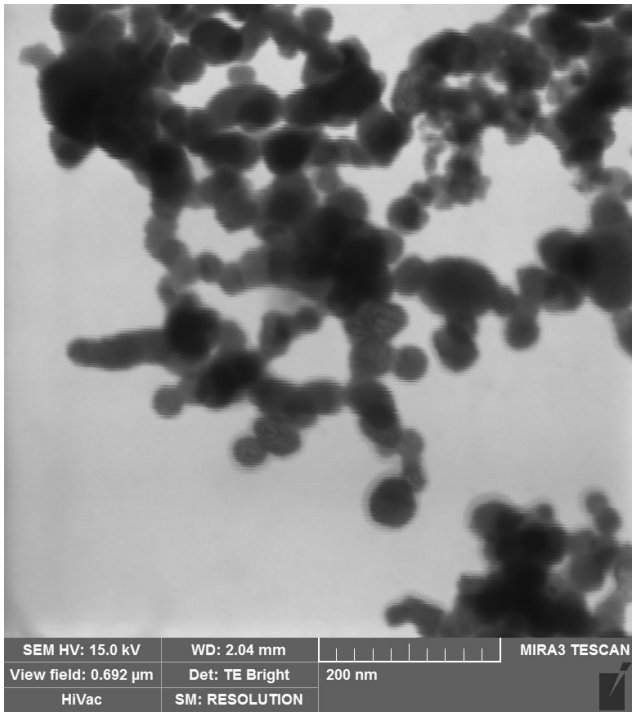

Fig.4 Scanning transmission electron micrograph of sample S3

When the results from all analytic techniques are combined, we can draw following conclusions: (i) As expected, the admixture of O_2 leads to the preferential formation of fully oxidised iron oxide phases: α-Fe_2O_3 and γ-Fe_2O_3. (ii) Hydrogen admixture, on the other hand, produces more material in a metallic state. However, the nanoproduct was well passivated and therefore, despite its immense specific surface area, not pyroforic. (iii) Adding nitrogen, well passivated product with even more metal (α-Fe percentage twice as much as with hydrogen admixture) was obtained. No iron nitride was detected.

The formation of core shell nanoparticles is probably a two step process. In the first one, the reducing atmosphere in the active discharge preferentially produces metallic nanoparticles. Then, as the nanoparticles are carried to the open end of the discharge tube, they gradually cool down and in the same time they experience the influence of the oxygen backdiffusing from the outer atmosphere. The lowered temperature and gradual introduction of oxygen prevents deep penetrating oxidation and only a thin protective layer of oxide forms. More quantitative explanation is not possible without detailed model including aerosol flow, diffusion, strong temperature gradients and homogeneous and heterogeneous chemistry. The hypothesis of two step process is supported by the fact, that we were not able [16] to passivate the nanoparticles using different experimental device which does not have the oxygen concentration gradient.

3. CONCLUSIONS

Iron based nanoparticles were synthesised in atmospheric pressure electrode-less microwave plasma jet - surfatron. Using several common admixtures to a main argon gas, we controlled the chemical and phase composition of produced nanoparticles.

In oxygen containing plasma, the product was preferentially formed of fully oxidised Fe_2O_3 allomorphs. In hydrogen containing atmosphere a greater abundance of metallic iron was observed. This iron nanopowder was found to be passivated by oxide shell, formed during later stages in the plasma afterglow. These results are consistent with common thermal process.

However, the addition of nitrogen did not produce iron nitride in contrast to thermal process, but iron/iron oxide core-shell nanoparticles with enhanced chemical stability.

ACKNOWLEDGEMENTS

This research has been supported by the project R&D centre for low-cost plasma and nanotechnology surface modifications CZ.1.05/2.1.00/03.0086 funded by European Regional Development Fund, by the project CEITEC - Central European Institute of Technology CZ.1.05/1.1.00/02.0068 from European Regional Development Fund and by the Czech Science Foundation P205/10/1374. The authors would like to thank Dušan Hemzal for Raman spectroscopy, Martin Haničinec for SEM micrograph and Mojmír Meduňa and Bohumil David for XRD measurements.

LITERATURE

[1] LU, A.H., SALABAS, E.L., SCHUETH, F. Magnetic nanoparticles: Synthesis, protection, functionalization, and application. *Angewandte chemie-international edition*, 2007, vol. 46, pp. 1222-1244.

[2] KIM, H., SIGMUND, W. Iron particles in carbon nanotubes. *Carbon*, 2005, vol. 43, pp. 1743-1748.

[3] HUBER, D.L. Synthesis, properties, and applications of iron nanoparticles. *Small*, 2005, vol. 1, pp. 482-501.

[4] VOLLATH, D. Plasma synthesis of nanopowders. *Journal of Nanoparticle Research*, 2008, vol. 10, pp. 39-57.

[5] MARIOTTI, D., SANKARAN, R.M. Perspectives on atmospheric-pressure plasmas for nanofabrication. *Journal of physics D: Applied Physics*, 2011, vol. 44, pp. 174023.

[6] SYNEK, P., JASEK, O., ZAJICKOVA, L., DAVID, B., KUDRLE, V., PIZUROVA, N. Plasmachemical synthesis of maghemite nanoparticles in atmospheric pressure microwave torch . *Materials Letters*, 2011, vol. 65, pp. 982-984.

[7] ZAJICKOVA, L., SYNEK, P., JASEK, O., ELIAS, M., DAVID, B., BURSIK, J. Synthesis of carbon nanotubes and iron oxide nanoparticles in MW plasma torch with Fe(CO)(5) in gas feed. *Applied Surface Science*, 2009, vol. 255, pp. 5421-5424.

[8] ZAJICKOVA, L., JASEK, O., ELIAS, M., SYNEK, P., LAZAR, L., SCHNEEWEISS, O. Synthesis of carbon nanotubes by plasma-enhanced chemical vapor deposition in an atmospheric-pressure microwave torch. *Pure and Applied Chemistry*, 2010, vol. 82, pp. 1259-1272.

[9] MOISAN, M., BEAUDRY, C., LEPRINCE, P. New HF device for production of long plasma columns at a high elektron-density. *Physics Letters*, 1974, vol. A 50, pp. 125-126.

[10] X'Pert HighScore Plus 2.0a Almelo, PANanalytica-B.V.

[11] Inorganic Crystals Structure Database, Hermannvon-Helmholtz-Platz, Eggenstein-Leopoldshafen, Karlsruhe, Germany.

[12] KIM, W., SUH, C.Y., CHO, S.W., ROH, K.M., KWON, H., SONG, K., SHON, I.J. A new method for the identification and quantification of magnetite-maghemite mixture using conventional X-ray diffraction technique. *Talanta*, 2012, vol. 94, pp. 348-352.

[13] JUBB, A.M., ALLEN H.C. Vibrational spectroscopic characterization of hematite, maghemite, and magnetite thin films produced by vapor deposition. *ACS Applied Materials & Interfaces*, 2010, vol. 2, pp. 2804-2812.

[14] DE FARIA, D.L.A., VENANCIO SILVA, S., DE OLIVEIRA M.T. Raman microspectroscopy of some iron oxides and oxyhydroxides. *Journal of Raman Spectroscopy*, 1997, vol. 28, pp. 873-878.

[15] WANG, C., BAER, D.R., AMONETTE, J.E., ENGELHARD, M.H., ANTONY, J., QIANG, Y. Morphology and electronic structure of the oxide shell on the surface of iron nanoparticles. *Journal of the American Chemical Society*, 2009, vol. 131, pp. 8824-8832.

[16] DAVID, B., PIZUROVA, N., SCHNEEWEISS, O., SANTAVA, E., JASEK, O., KUDRLE, V. alpha-Fe nanopowder synthesised in low-pressure microwave plasma and studied by Mossbauer spectroscopy . *Journal of Physics Conference Series*, 2011, vol. 303, pp. 012090.